Flotats, X. and Puigjaner, L. (1994). Modeling anaerobic digestion proceses using a discrete bivariant distribution of gas bubbles and biomass aggregate sizes. In *Ed. Sup Yoon (Ed) Korean Institute of Chemical Engineers. The 5th International Symposium on Process Systems Engineering.* ISBN 89950005 1 1 94570. Vol. 1, pp 655-662.

# Modelling Anaerobic Digestion Processes Using a Discrete Bivariant Distribution of Gas Bubble and Biomass Aggregate Sizes

X. Flotats[1], L. Puigjaner[2]

[1] Dep. of Environmental and Soil Sciences. Universitat de Lleida. Rovira Roure 177, 25006 Lleida, Spain*.

[2] Dep. of Chemical Engineering. Universitat Politècnica de Catalunya. Diagonal 647, 08028 Barcelona, Spain.

## ABSTRACT

A structured model, based on the dynamics of a discrete bivariant distribution of sizes of bacterial aggregates and gas bubbles has been developed. It offers a methodological way to achieve a mathematical synthesis of empirical knowledge about some phenomena involved in anaerobic filter reactor performance such as aggregation, fragmentation, sedimentation, surface colonization and biofilm removal by fluid motion.

Simulations allow the detection of some limit situations such as hydraulic retention time for maximum biogas production and the minimum retention time for reactor activity. An oriented support anaerobic filter pilot plant data related to particles caracterization, methane production and soluble Q.O.D. removal have been used to validate the model with satisfactory results.

## INTRODUCTION

Anaerobic digestion processes based on biofilm and/ or bacterial aggregates formation are difficult to model, and they are likely to be designed on the basis of empirical evidence. This difficulty comes from the need of taking into consideration all phenomena involved: biomass aggregation, growth, fragmentation, substrate consumption, gas bubble formation and aggregates transport by settling or by flotation caused by attached bubbles. If reactors are of the anaerobic filter type, then surface colonization to create biofilms, substrate consumption, new bubbles formation, growth and removal will also be considered.

Some empirical models for anaerobic filter reactors have been developed. Those models are useful to fit experimental data, but do not allow reactor performance explanation at all.

For anaerobic fixed film reactors, activity is considered to be due to microbial biofilm developed over the support matrix. This clearly requieres the biofilm to be stationary and the net biomass grown fraction to be rapidly sloughed and washed-out, in order not to consider its activity. For low retention time fermentors, models based on biofilm kinetics allow to explain and simulate reactor performance with satisfactory results[1].

For upflow anaerobic fixed film reactors with high retention time or discontinously loaded, biofilm sloughing or attrition may result in rather large microbial aggregate fragments that are retained in the reactor. Those aggregates consume subtrate, grow, fragment into lower aggregate sizes, are transported by settling and upwards by fixed bubbles or by fluid flow, and colonize new surfaces where a biofilm will be developed.

Biofilm and free microbial cell interaction have been studied by some researchers[2] and non-uniformity in free microbial aggregate sizes has been experimentally established for some types of bioreactors[3,4].

Aggregate size influences substrate uptake effectiveness, growth, settling velocity and reactor retention capacity. Although some experiences proved distribution

* Author to whom all correspondence should be addressed

size significance, few works have attempted to model its dynamics distribution[3,5,6]. Among those works, that of Beeftink and Van den Heuvel[6] provides a powerful structured model and was a basic reference to develop some aspects of the present work.

During the experimental works, treating liquid fraction of pig waste, over an upflow anaerobic filter with vertically oriented support, disposed as shown in Fig.1, suspended microbial aggregates moving in the interstitial support spaces and modifying reactor performance were appreciated[8]. A simplified semi-empirical model based on Contois kinetics and the assumption of biomass and substrate homogeneous distribution, due to gas mixing, was developed. This model fits the pilot plant data related to gas production and effluent depuration but it cannot answer why the minimum retention time due to suspended biomass wash-out is 2.3 days or why effluent particles show low settling velocities over the retention time when gas production is maximum (4.8 days).

In order to overcome the empirical model limitations, a structured model based on the dynamics of a discrete bivariant distribution of bacterial aggregates and gas bubbles was developed. Its main guidelines are presented here.

## MODELLING FRAMEWORK

A particle will be defined as integrated by solid (bacterial aggregate) and gas (biogas bubble) phases. Aggregates and bubbles will be postulated to have spherical geometry. Biofilms will be postulated to have the same intrinsic properties as free aggregates, such as density, biomass concentration or substrate diffusivity, but fixed to reactor support with cylindrical geometry. Gas will be postulated to be produced in thé aggregates and biofilms.

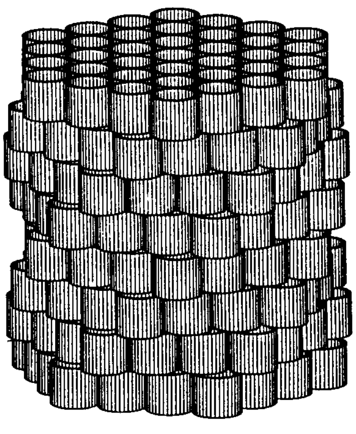

Fig.1. Configuration of the vertically oriented support.

Rates involved in final partial differential equations are defined in Table 1 and explained below.

### Particles distribution setting up

Free aggregate diameters $d$ belong to a total number of $m$ size categories with class width $w_a$. Each diameter category is represented by $d^i$, equal to the median of that class. An aggregate of diameter $d$ belongs to the category $(i,0)$ if $d \in [d_i - \frac{w_a}{2}, d_i + \frac{w_a}{2})$, $d_i = (i - \frac{1}{2})w_a$, $i = 1, 2, ..., m$.

Free bubble diameters $d$ belong to a total number of $n$ size categories with class width $w_b$. Each diameter category is represented by its median $d^j$. A bubble of diameter $d$ belongs to the category $(0,j)$ if $d \in [d^j - \frac{w_b}{2}, d^j + \frac{w_b}{2})$, $d^j = (j - \frac{1}{2})w_b$, $j = 1, 2, ..., n$.

A particle belongs to the category $(i,j)$, $i = 0, 1, ..., m$, $j = 0, 1, ..., n$, if its biomass aggregate belongs to the $(i,0)$ category and its gas bubble belongs to the category $(0,j)$.

Particles concentration by volume, for each category, will be noted by $C_i^j$, $i = 0, 1, ..., m$, $j = 0, 1, ..., n$. The diagram of particles concentration distribution by categories is represented in Fig.2.

The aggregate fraction for particles of $(i,j)$ category is defined by $f_i^j = \frac{(d_i)^3}{(d^j)^3 + (d_i)^3}$ and the bubble fraction by $(1 - f_i^j)$.

For each category, settling or upward particle velocity $u_{oi}^j$ is calculated by fixing biomass aggregates and gas densities ($\rho_s$ and $\rho_g$ respectively) and using appropriate correlations for particles and bubbles.

### Substrate consumption

Substrate consumption rate for overall $(i,j)$ category particles will be noted $\lambda_i^j$ and the rate for the biofilm will be noted $\lambda_x$. The Monod type kinetics, $\mu_M = \frac{\hat{\mu} C_B}{K_s + C_B}$, and constancy of $Y$, the biomass yield on the substrate, $D_x$, the effective diffusivity of the substrate in an aggregate and $X_o$, the biomass concentration in an aggregate, will be postulated.

The substrate consumption rate per unit of aggregate volum varies with the aggregate size, the bulk-liquid substrate concentration $C_B$ and the relative aggregate/fluid velocity due to internal and external substrate transport resistances. This variation is caracterized by the effectiveness factor $\eta$, $\eta_i^j$ for $(i,j)$ category particles

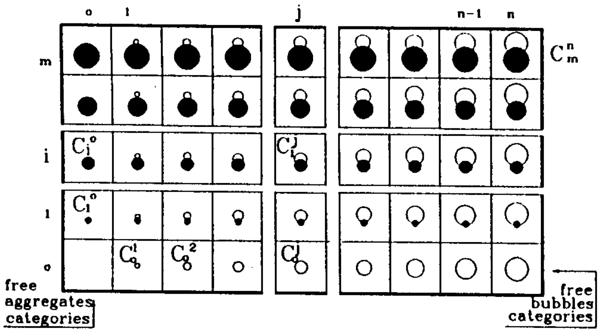

Fig.2. Diagram of the particle concentration bivariant distribution by aggregate and bubble diameters.

and $\eta_x$ for biofilm, defined as the ratio between the actual consumption rate of an aggregate and the rate that would be in the absence of transport limitations. This factor will be calculated by solution approximation of the diffusion and reaction equation in a given aggregate geometry, including external transport limitations as a boundary condition[8].

## Growth

The growth of particles is due to the growth of aggregate fraction, due to synthesized biomass from substrate consumption, and the growth of bubble fraction, due to the gaseous metabolites produced.

For the $(i, j)$ category, growth is represented as an increase in the concentration $C_i^j$ due to the transition of particles from the $(i-1, j-l)$ category, and a decrease due to the transition of $(i, j)$ particles to the category $(i+1, j+k)$ of bigger sizes (see diagram on Fig.3).

Substrat consumption by biofilm implies, as spherical aggregates, a growth of biofilm volume $V_x$. Biofilm gas production is postulated to increase free bubbles concentration of the $(0, 1)$ category.

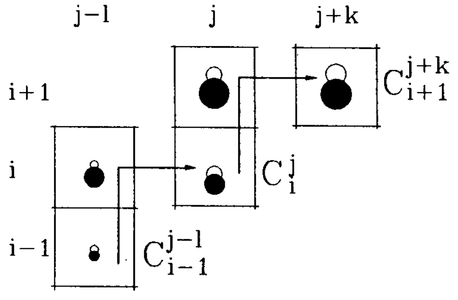

Fig.3. Diagram of particles growth model.

## Particle fragmentation

Production of gaseous metabolites in the aggregates may reduce microbial cell cohesion and leads to particle disintegration. Edelstein and Hadar[5] define fragmentation rate as a function of fluid shear stress and Beeftink and Van den Heuvel[6] propose that this rate is a function of substrat consumption rate and biomass concentration in the aggregates, which decreases with bacterial decay. In order to simplify expressions no decay rates will be considered and it will be postulated that fragmentation rate for a given category $(p, j)$ is proportional to substrate consumption rate $\lambda_i^j$ and particle gaseous fraction $(1 - f_p^j)$, with $f_{fr}$ as a constant proportionality factor.

The fragmentation process for a given $(p, j)$ category is represented by a decrease in its concentration, an increase in the $(0, j)$ free bubbles category and an increase in free aggregates of lower size categories (see diagram in Fig.4). As in Beeftink and Van den Heuvel model[6], it will be postulated that an "$a$" fraction of a disintegrated aggregate is split into two halves, while the remaining part $(1 - a)$ is incorporated in the smallest type of free aggregate $(1, 0)$.

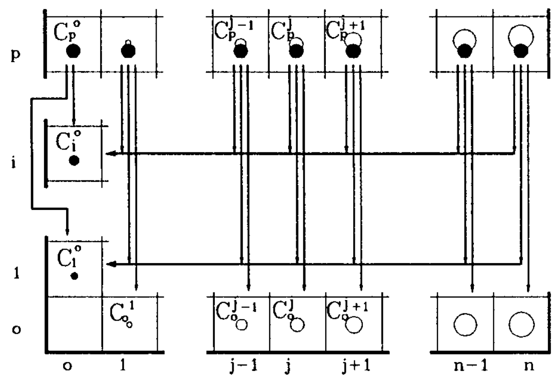

Fig.4. Diagram of particles fragmentation model.

## Particle axial collisions with support

There are experimental evidences that upward particle axial collisions with support enhace phase separation and aggregates confination. It will be postulated that all collisions lead to phase separation. The collision probability $P_x$, per unit of lenght, will be calculated as the ratio between the support section and the free flow section $\overline{S}_x$, if there are distribution support changes at the given height of the reactor. $P_x$ value is 0.19 each 30 mm of height, for Fig.1 support distribution.

Table 1. Rates involved in model definition

| | Particles | Biofilm |
|---|---|---|
| Growth | $(\Gamma_{gr})_i^j = \mu_M (d_i)^3 \left( \eta_{i-1}^{j-l} \frac{C_{i-1}^{j-l}}{(d_i)^3-(d_{i-1})^3} \frac{\mathbf{f}_{i-1}^{j-l}}{\mathbf{f}_i^j} - \eta_i^j \frac{C_i^j}{(d_{i+1})^3-(d_i)^3}\right),$<br>$i=1,2,...,m-1; \quad j=0,1,...,n$ | $\Gamma_{gr} = \eta_x V_x \mu_M$ |
| Fragmentation | $(\Gamma_{fr})_p^j = -f_{fr}\lambda_p^j(1-\mathbf{f}_p^j)C_p^j,$<br>$p=1,2,...,m; \quad j=1,2,...,n$<br>$(\Gamma_{fr})_i^0 = a\sum_{j=1}^{n}\sum_{p=c}^{d} \mathbf{f}_p^j (\Gamma_{fr})_p^j, \quad i=1,2,...,m$<br>$(\Gamma_{fr})_1^0 = (1-a)\sum_{j=1}^{n}\sum_{p=1}^{m} \mathbf{f}_p^j (\Gamma_{fr})_p^j$<br>$(\Gamma_{fr})_0^j = \sum_{p=1}^{m}(1-\mathbf{f}_p^j)(\Gamma_{fr})_p^j, \quad j=1,2,...,n$ | |
| Attachment | $(\Gamma_{at})_i^j = -\frac{1}{\overline{V}_x}\Gamma_{at}, \quad i=1; \quad j=0$<br>$(\Gamma_{at})_i^j = 0, \quad i=0,2,3,...,m; \quad j=0,1,...,n$ | $\Gamma_{at} = \varphi_1^0 \overline{S}_x P_T P_f$ |
| Detachment | $(\Gamma_{dt})_i^j = -\frac{1}{\overline{V}_x}\Gamma_{dt}, \quad i=1; \quad j=0$<br>$(\Gamma_{dt})_i^j = 0, \quad i=0,2,3,...,m; \quad j=0,1,...,n$ | $\Gamma_{dt} = -\frac{(S_x(\delta_x)-S_x(\delta))u_1^0\overline{S}_x(\delta_x)\varepsilon_p}{\overline{S}_x(\delta)-\overline{S}_x(\delta_x)(1-\varepsilon_p)},$<br>$\delta < \delta_x$<br>$\Gamma_{dt} = 0, \quad \delta \geq \delta_x$ |
| Axial collision with support | $(\Gamma_{ac})_i^j = P_x u_i^j C_i^j, \quad u_i^j < 0,$<br>$(\Gamma_{ac})_i^j = 0, \quad u_i^j \geq 0,$<br>$i=1,2,...,m; \quad j=1,2,...,n$<br>$(\Gamma_{ac})_i^0 = \sum_{j=1}^{n} \mathbf{f}_i^j (\Gamma_{ac})_i^j, \quad i=1,2,...,m$<br>$(\Gamma_{ac})_0^j = \sum_{i=1}^{m}(1-\mathbf{f}_i^j)(\Gamma_{ac})_i^j, \quad j=1,2,...,n$ | |
| Biofilm gas production | $(\Gamma_{bg})_i^j = B_g \frac{\lambda_x}{\overline{V}_x}, \quad i=0; \quad j=1$<br>$(\Gamma_{bg})_i^j = 0, \quad i=0,2,3,...,m; \quad j=0,1,...,n$ | |
| Substrate consumption | $\lambda_i^j = \eta_i^j \mu_M \frac{X_0}{Y\varepsilon_p} \mathbf{f}_i^j C_i^j,$<br>$i=1,2,...,m; \quad j=0,1,...,n$ | $\lambda_x = \eta_x \frac{S_x}{\overline{S}_x}\frac{X_0}{Y\varepsilon_p}\mu_M$ |
| Vertical transport | $(\Gamma_{tr})_i^j = \frac{\partial \varphi_i^j}{\partial x}, \quad \varphi_i^j = u_i^j C_i^j, \quad \varepsilon_p = 1-\sum_{j=0}^{n}\sum_{i=0}^{m} C_i^j,$<br>$u_i^j = u_{oi}^j \varepsilon_p^{n_i^j-1} - \sum_{k=0}^{m}\sum_{l=0}^{n} u_{ok}^l \varepsilon_p^{n_k^l-1} C_k^l + \frac{Q(t)}{\overline{S}_x}$ | |

Axial collision for $(i,j)$ category particles is represented by a concentration decrease in this category and an increase in $(i,0)$ and $(0,j)$ categories.

Bacterial attachment to biofilm

Biofilm development on a surface exposed to a fluid flow is the net result of several processes: Transport of microbial cells to surface, microorganisms attachment, growth on the surface and partial detachment caused by fluid shear stress[2].

The rate of increase in the biofilm volume $V_x$ at a given reactor height, by attachment of microbial cells assumed to belong to the $(1,0)$ category, is postulated to be the product of the particles flux $\varphi_1^0$, its probability to contact biofilm surface $P_T$ and the sticking efficiency $P_f$, estimated as a function of shear stress[7]. An increase in the biofilm volume by cells attachment leads to a decrease in $(1,0)$ particle concentration.

Biofilm detachment

Once the biofilm thickness $\delta_x$ exceeds the laminar sublayer thickness $\delta$, shear stress increases dramatically and so does biofilm removal rate[7]. Although studies have shown that removal, by attrition or sloughing, is a continous process during biofilm development[2], in order to simplify expressions it will be postulated that there is a detachment when $\delta < \delta_x$. The biofilm fraction placed out of $\delta$ bound will be removed and incorporated into suspended biomass as $(1,0)$ category particles.

Vertical transport of particles

Vertical transport of particles will be modelled by evolution equations of a suspension composed by inert particles of various diameters and densities, using Richardson-Zaki equation and taking into account that the velocity for each category is controlled by the overall particle concentration at a given height of the reactor. It will be assumed that every particle has spherical geometry.

Setting-up the model

Evolution equations for the particle concentration $C_i^j$ and the bulk-liquid substrate concentration $C_B$ in a differential volum of height $dx$ and section $\overline{S}_x$, and the evolution equation for the biofilm volume $V_x$ of height $dx$ and section $S_x$, at a given height $x$ in a $L$ height reactor, with the rates as defined in Table 1, are

$$\frac{\partial C_i^j}{\partial t} = (\Gamma_{tr})_i^j + (\Gamma_{gr})_i^j + (\Gamma_{fr})_i^j + (\Gamma_{at})_i^j + (\Gamma_{dt})_i^j + (\Gamma_{ac})_i^j + (\Gamma_{bg})_i^j,$$

$$\frac{\partial V_x}{\partial t} = \Gamma_{gr} + \Gamma_{at} + \Gamma_{dt},$$

$$\frac{\partial C_B}{\partial t} = \frac{\partial v C_B}{\partial x} - \sum_{i=1}^{m}\sum_{j=0}^{n} \lambda_i^j - \lambda_x,$$

$$i = 0,1,...m, \quad j = 0,1,...n, \quad (i,j) \neq (0,0),$$

$$x \in [0,L],$$

with the appropriate boundary and initial conditions for a given reactor configuration[8].

RESULTS AND DISCUSSION

Thirty days process numerical simulations have been obtained, using a 7x7 particles bivariant distribution and the parameter values and initial conditions showed at Table 2.

Table 2. Parameter values and initial conditions used for numerical simulations.

| | | |
|---|---|---|
| $C_{Bin}$ | 7.0 | kg QOD·m$^{-3}$ |
| $Q(t)$ | 0.0794·$\Theta^{-1}$ | m$^3$·day$^{-1}$ |
| $\Theta$ | 0.2, 1.0, 1.8,..., 9.8 | days |
| $d_m$ | 0.3·10$^{-3}$ | m |
| $d^n$ | 1.0·10$^{-3}$ | m |
| $m$ | 7 | |
| $n$ | 7 | |
| $X_o$ | 150 | kg biomass·m$^{-3}$ |
| $Y$ | 0.12 | kg biomass·(kg QOD)$^{-1}$ |
| $\hat{\mu}$ | 0.25 | day$^{-1}$ |
| $K_s$ | 120 | kg QOD·m$^{-3}$ |
| $D_\ell$ | 0.5·10$^{-7}$ | m$^2$·s$^{-1}$ |
| $D_s$ | 0.75·10$^{-8}$ | m$^2$·s$^{-1}$ |
| $\nu_\ell$ | 7.73·10$^{-7}$ | m$^2$·s$^{-1}$ |
| $\rho_g$ | 1.15 | kg·m$^{-3}$ |
| $\rho_\ell$ | 1000 | kg·m$^{-3}$ |
| $\rho_s$ | 1030 | kg·m$^{-3}$ |
| $B_g$ | 0.75 | m$^3$ gas·(kg QOD)$^{-1}$ |
| $f_{fr}$ | 0.7 | (kg QOD)$^{-1}$ |
| $a$ | 0.6 | |
| $P_x$ | 0.19 | |
| $L$ | 2 | m |

Initial conditions ($x \in [0,L]$):

| | |
|---|---|
| $C_i^j(x,0) = 2.0 \cdot 10^{-3}$ | $i=1$, $j=0$ |
| $C_i^j(x,0) = 0$ | $i=0,2,3,...m$, $j=0,1,...n$ |
| $S_x(x,0) = 1 \cdot 10^{-4}$ m$^2$ | $\delta_x(x,0) = 25$ m$^{-6}$ |
| $\overline{S}_x(x,0) = 3.96 \cdot 10^{-2}$ m$^2$ | |
| $C_B(x,0) = 7$ kg QOD·m$^{-3}$ | |

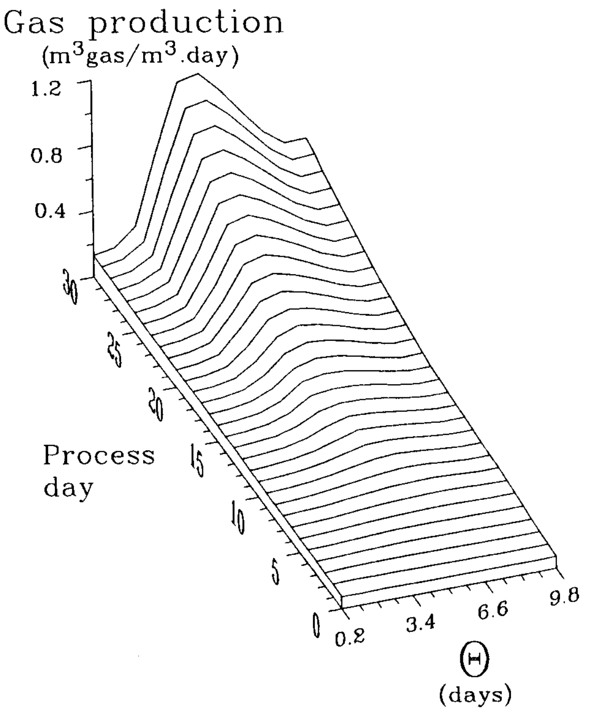


Fig.5. Evolution of simulated gas production.

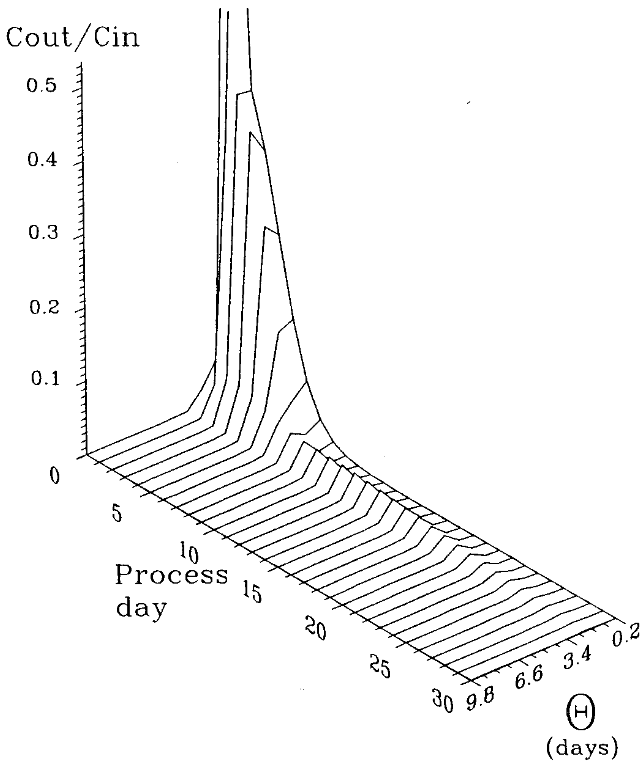


Fig.6. Simulated evolution of the ratio between effluent aggregate concentration (Cout) and the overall aggregate fraction concentration in the reactor (Cin), for the different retention times.

Kinetic parameters $\widehat{\mu}$, $K_s$ and $B_g$ have been estimated by using the simplified model based on Contois kinetics above mentioned, and fitting the pilot plant data related to gas production and effluent depuration. Fragmentation parameter values, $f_{fr}$ and $a$, have been taken as in [6]. Values for reactor configuration parameters $L$, $P_x$ and $\overline{S}_x$, with 0.8 as initial support porosity, have been calculated from the experimental reactor used.

Solutions have been approached by finite differences using the off-center explicit method and taking 50 nodes uniformly distributed along the reactor height.

Fig.5 shows evolution of gas production and Fig.6 shows the ratio between effluent aggregate concentration and the overall aggregate fraction concentration in the reactor.

Numerical simulations show aggregates wash-out for retention times below 2.2 days that are consistent with experimental results. Reactor activity is due to biofilm exclusively at high loading rates (i.e. low retention times, at or below 2.2 days). Simulated biogas production presents a maximum near 4.8 days retention time as obtained in pilot plant data.

Maximum biofilm thickness is obtained at 4.2 days retention time. Net biofilm growth is limited by fluid shear stress and microbial cell detached are washed-out rapidly below 4.2 days.

Net biofilm growth is limited by bulk-liquid substrate transport and aggregates competition in substrate uptake above 4.2 days. Aggregates reach the upper part of the reactor by flotation and particles with bubbles, poor in settling properties, are found in the effluent.

Real averaged QOD depuration has been slightly greater than in numerical results above 5 days retention time. That may be due to the low biomass on substrate yield $Y$ taken in the simulations.

## CONCLUSIONS

A structured model based on the dynamics of a discrete bivariant distribution of particles, the biofilm dynamics and their interaction has been developed. Although multiple simplification assumptions and postulates are needed, it offers a methodological way to formulate hypotheses, to detect some limit situations and to achieve a mathematical synthesis of empirical knowledge about the considered phenomena. The results obtained by numerical simulation, applying boundary conditions for an upflow anaerobic filter reactor with oriented support, show the same pilot plant tendencies, validating the model qualitatively.

## REFERENCES


[1] Rittmann, B.E. and P.L. McCarty, Biotechnology and Bioengineering, 22 (1980) 2359.

[2] Trulear, M.G. and W.G. Characklis, Journal WPCF, 9, 54 (1982) 1288.

[3] Atkinson, B. and F. Ur-Rahman, Biotechnology and Bioengineering, 21 (1979) 221.

[4] Beeftink, H. and P. Satugaard, Applied and Environ. Microbiology, 52 (1986) 1139.

[5] Edelstein, L. and Y. Hadar, Journal Theor. Biol., 105 (1983) 427.

[6] Beeftink, H. and J.C. Van den Heuvel, The Chemical Engineering Journal, 44 (1990) 1.

[7] Bryers, J.D., Biotechnology Progress, 3, 2 (1987) 57.

[8] Flotats, X., "Liquid fraction pig waste treatment by an anaerobic filter with oriented support", Ph.D. Thesis, Universitat Politècnica de Catalunya (1993).